Modeling the Effects of Electric Fields on Nerve Fibers: Influence of Tissue Electrical Properties

Warren M. Grill, Jr., *Member, IEEE*

***Abstract*— The effects of anisotropy and inhomogeneity of the electrical conductivity of extracellular tissue on excitation of nerve fibers by an extracellular point source electrode were determined by computer simulation. Analytical solutions to Poisson's equation were used to calculate potentials in anisotropic infinite homogeneous media and isotropic semi-infinite inhomogeneous media, and the net driving function was used to calculate excitation thresholds for nerve fibers. The slope and intercept of the current-distance curve in anisotropic media were power functions of the ratio and product of the orthogonal conductivities, respectively. Excitation thresholds in anisotropic media were also dependent on the orientation of the fibers, and in strongly anisotropic media ($\sigma_z/\sigma_{xy} > 4$) there were reversals in the recruitment order between different diameter fibers and between fibers at different distances from the electrode. In source-free regions of inhomogeneous media (two regions of differing conductivity separated by a plane boundary), the current-distance relationship of fibers parallel to the interface was dependent only on the average conductivity, whereas in regions containing the source the current-distance relationship was dependent on the individual values of conductivity. Reversals in recruitment order between fibers at different distances from the electrode and between fibers of differing diameter were found in inhomogeneous media. The results of this simulation study demonstrate that the electrical properties of the extracellular medium can have a strong influence on the pattern of neuronal excitation generated by extracellular electric fields, and indicate the importance of tissue electrical properties in interpreting results of studies employing electrical stimulation applied in complex biological volume conductors.**

***Index Terms*—Anisotropy, current-distance relationship, extracellular field, inhomogeneity, neural stimulation.**

NOMENCLATURE

$\Phi_{(x,y,z)}$	Extracellular potential (mV).
I	Current magnitude (μA).
σ	Electrical conductivity of homogeneous isotropic medium (S/cm).
σ_z	Longitudinal conductivity in anisotropic medium (S/cm).
$\sigma_{xy} = \sigma_x = \sigma_y$	Transverse conductivity in anisotropic medium (S/cm).
$\sigma_1(\sigma_2)$	Electrical conductivity of region 1 (2) of inhomogeneous medium (S/cm).
a	Distance from source to plane interface in an inhomogeneous medium (cm).
l	Distance from fiber to plane interface in an inhomogeneous medium (cm).
n	Index of node number along cable model of nerve fiber (1..21).
$V_{m(n,t)}$	Transmembrane voltage (mV).
$f(n)$	Second difference of the extracellular potential at node n (mV).
G_i	Intracellular conductance ($1/\Omega$).
$\Psi_{(n,j,t)}$	Transmembrane potential generated at compartment n by a unit step of current injected at compartment j (Ω).
$I_{\text{thr-ext}}(n, \text{PW})$	Threshold current to excite node n with an extracellular stimulus of duration PW (μA).
$I_{\text{thr-int}}(n, \text{PW})$	Threshold current to excite node n with an intracellular stimulus of duration PW (μA).
PW	Duration of rectangular stimulus pulse (μs).
I_o	Intercept in current-distance equation (μA).
k	Slope in current-distance equation (μA/mm^2).

Manuscript received October 19, 1998; revised January 7, 1999. This work was supported by the National Science Foundation (NSF) Biomedical Engineering and Research to Aid Persons with Disabilities Program (BES-9709488) and by the Department of Veterans Affairs, Rehabilitation Research and Development Service Center of Excellence in FES.

The author is with the Department of Biomedical Engineering, Case Western Reserve University, Applied Neural Control Lab, CB Bolton Building., Room 3480, Cleveland OH 44106-4912 USA (e-mail: wmg@po.cwru.edu).

Publisher Item Identifier S 0018-9294(99)05767-5.

I. INTRODUCTION

THE changes in transmembrane potential generated in neurons by an extracellular electric field depend on the spatial and temporal properties of the field as well as the electrical properties and geometry of the neuron [8]. In this study, the effects of the electrical properties of the extracellular medium on the pattern of neuronal excitation generated by an extracellular electric field are analyzed. The influence of anisotropy and inhomogeneity of the conductivity on the relationship between the threshold current and the electrode to fiber distance (current-distance relationship) is determined. These electrical properties are a common feature of biological tissues [12], [14], thus the results of this study are relevant for extracellular activation of the nervous system throughout the body.

Previous models of neuronal excitation with extracellular electric fields range from simple point sources in homogeneous, isotropic media, to complex three-dimensional models incorporating inhomogeneous and anisotropic volume conductors. Simple models have been used to study the effects of stimulus waveform on excitation [16], [19], [20], [27], [39],

as well as to compare different solutions for predicting the neural response to an imposed field [2], [38], [43], [53]. More complex models include realistic representations of the tissue geometry and electrical properties and electrode geometries suited for a specific application. For example, investigators have modeled extracellular stimulation of peripheral nerve fibers [3], [51], electrical stimulation of the spinal cord [7], [9], [45], [47], and electrical stimulation of the cochlear nerve [11], [13]. While these models provide considerable insight into specific applications, it is difficult to separate the effects due to the specific electrical properties of the tissue from purely geometrical effects.

The purpose of this investigation was to present results at a level of complexity intermediate between an infinite homogeneous isotropic medium and case specific numerical models. The influence of electrical anisotropy of the extracellular tissue was considered by modeling a higher conductance along one axis and lower, equal conductances along the orthogonal axes. Such a medium is representative of a number of biological tissues where the ratio of longitudinal conductivity to transverse conductivity may be as high as ten to one including skeletal muscle [15], peripheral nerve [1], [49], and cerebral and spinal white matter [28], [37]. The influence of inhomogeneity of the electrical conductivity was considered by modeling a planar interface between two semi-infinite media with different conductivities. Conductivity boundaries create secondary sources during application of exogenous electric fields [34]. This model is representative of interfaces between different tissue types, such as found in the cerebellum [31], hippocampus [23], and neocortex [22], [32], [41], as well as in peripheral nerve [50]. The results of this study demonstrate that the electrical properties of the extracellular tissue can have a strong effect on the pattern of neuronal excitation, including reversals in the recruitment order between fibers of differing diameter and at different distances from the electrode. Preliminary results of these studies have been presented in abstract form [18].

II. Methods

Computer-based models were used to determine the effects of the electrical properties of the extracellular tissue on the threshold current for excitation of model nerve fibers with an extracellular point source electrode. Analytical solutions to Poisson's equation were used to calculate the extracellular potentials in infinite homogeneous anisotropic media and isotropic semi-infinite inhomogeneous media, assuming that the tissue was purely resistive [36]. The potentials were then combined with the net driving function to calculate the threshold current for activation of a particular nerve fiber [53]. This was repeated to obtain a relationship between the threshold current and the electrode to fiber distance (current-distance curve) for different diameter fibers (10 μm and 20 μm) in different media.

A. Calculation of Extracellular Potentials

In a homogeneous isotropic media with conductivity σ the potential, Φ, generated at a point (x, y, z) by a point current source I at the origin is given by

$$\Phi(x,y,z) = \frac{I}{4\pi\sigma\sqrt{x^2+y^2+z^2}}. \tag{1}$$

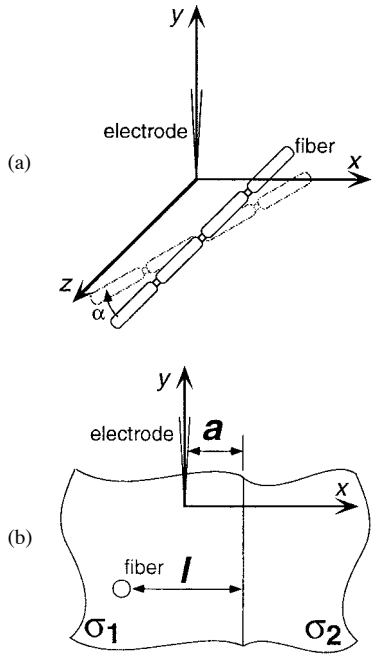

Fig. 1. Geometries of electrode, nerve fiber, and tissue. (a) Geometry in infinite anisotropic medium with longitudinal conductivity (σ_z) greater than transverse conductivity ($\sigma_x = \sigma_y$). The electrode was positioned at the origin and the fiber lay in a plane parallel to the x-z plane at angle α to the z-axis. (b) Geometry in semi-infinite inhomogeneous media with two regions of differing conductivity (σ_1, σ_2) separated by a plane boundary parallel to the y-z plane. The electrode was positioned at the origin, distance a from the interface, and the fiber lay in a plane parallel to the x-z plane, distance l from the interface.

A coordinate transform [29], [52] was used to determine the potential in anisotropic media with different conductivities in the longitudinal and transverse directions [Fig. 1(a)]. The potential generated by a point current source I at the origin in a two-dimensionally anisotropic medium with longitudinal conductivity σ_z and transverse conductivity $\sigma_x = \sigma_y = \sigma_{xy}$ is

$$\Phi(x,y,z) = \frac{I}{4\pi\sqrt{x^2\sigma_{xy}\sigma_z + y^2\sigma_{xy}\sigma_z + z^2\sigma_{xy}^2}}. \tag{2}$$

The method of images [34] was used to determine the potential generated in a medium containing two regions with different conductivities [Fig. 1(b)]. The potential generated at point (x, y, z) in a semi-infinite isotropic medium with conductivity σ_1 separated by a plane boundary from another semi-infinite isotropic medium with conductivity σ_2 by a point current source I at the origin in region 1 is

$$\Phi(x,y,z) = \frac{I}{4\pi\sigma_1}\left[\frac{1}{\sqrt{x^2+y^2+z^2}} + \frac{(\sigma_1-\sigma_2)}{(\sigma_1+\sigma_2)\sqrt{(2a-x)^2+y^2+z^2}}\right] \tag{3}$$

where a is the distance from the source to the boundary [Fig. 1(b)]. The potential at point (x, y, z) in region 2 from

a point current source I in region 1 is given by

$$\Phi(x,y,z) = \frac{I}{2\pi(\sigma_1+\sigma_2)\sqrt{x^2+y^2+z^2}}. \tag{4}$$

B. Determination of Fiber Response to Imposed Field

A 21-compartment passive cable model was used to represent a myelinated nerve fiber. The transmembrane potential, $V_m(n,t)$ generated in the passive model nerve fiber by the extracellular field was calculated using the net driving function [53], which provides an analytical expression (5) for $V_m(n,t)$ based on a weighted summation of the second spatial difference of the extracellular potentials, $f(n) = [\Phi(n-1) - 2\Phi(n) + \Phi(n+1)]$

$$V_m(n,t) = \Psi(n,n,t)\cdot G_i\left\{ f(n) + \sum_{j\neq n} \frac{\Psi(n,j,t)}{\Psi(n,n,t)} f(j) \right\} \tag{5}$$

where G_i is the intracellular conductance and $\Psi(n,j,t)$ is the transmembrane potential at compartment n generated by a unit step of current injected at compartment j. The calculation of these terms is described in detail in Warman *et al*. [53].

The threshold current to excite a particular node, n, of the neuron with an extracellular electrode is given by (6) where $I_{\text{thr-int}}(n,\text{PW})$ is the intracellular current amplitude required to excite node n with a pulse of duration PW, and the subscript "u" on the $f(n)$ terms indicates that the magnitude of $f(n)$ is generated with a unit of extracellular current [53].

$$I_{\text{thr-int}}(n,\text{PW}) = \frac{I_{\text{thr-int}}(n,\text{PW})}{G_i(n)\cdot\left\{ f_u(n) + \sum_{j\neq n} \frac{\Psi(n,j,\text{PW})}{\Psi(n,n,\text{PW})} f_u(j) \right\}}. \tag{6}$$

This relation was used to generate curves of the minimum (threshold) current to excite any node of the fiber as a function of electrode to fiber distance (current-distance curves) in different media.

III. Results

A. Validation of Threshold Estimates

Threshold currents estimated using the net driving function [(6)] were compared to threshold currents calculated (±1%) using a model of the active nerve fiber [48]. Thresholds for excitation of 10-μm and 20-μm nerve fibers with a 100-μs monophasic rectangular pulse as a function of the electrode to fiber distance in a homogeneous isotropic medium ($\sigma = 0.018$ S/cm) are shown in Fig. 2. The net driving function provided an accurate estimate of the threshold current. The root mean square errors over the current-distance curves were 0.026 mA and 0.023 mA for the 10-μm and 20-μm fibers, respectively. The maximum errors were −2.4% (10 μm) and −3.5% (20 μm) when expressed as a percentage of the threshold current obtained with the active model. These data demonstrate that the net driving function provided estimates of the current threshold for extracellular stimulation within 4% of the computed value. Further, both the shape of the current-distance curve and the relative magnitude of the currents required for excitation correspond well to experimental measurements of nerve fiber excitation [4], [5], [40], [46], [21], [54].

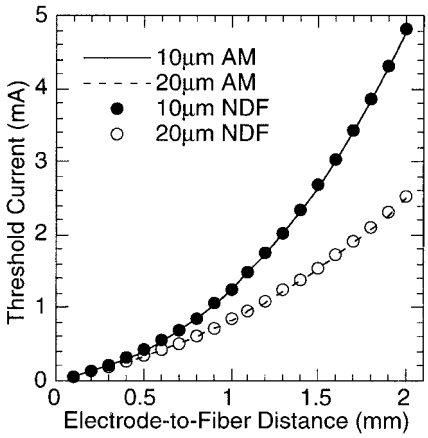

Fig. 2. Comparison of the threshold currents for excitation of 10-μm and 20-μm model nerve fibers in an infinite, homogeneous ($\alpha = 0.018$ S/cm) isotropic medium either calculated by solution of the nonlinear differential equations describing the active model (AM) or estimated using the net driving function (NDF).

B. Anisotropic Extracellular Medium

Two-dimensional anisotropy (i.e., $\sigma_x = \sigma_y < \sigma_z$) arises in biological conductors which consist of bundles of long, parallel elements (e.g., nerve fibers, muscle fibers). The influence of anisotropy on the patterns of excitation of nerve fibers by an extracellular point source electrode was determined for varying anisotropy ratios and nerve fiber orientations.

1) Influence of Anisotropy on the Current-Distance Relationship: The relationship between the threshold current and the electrode to fiber distance was dependent on the principal conductivities of the extracellular medium as well as the orientation of the fibers with respect to the principal axes. Current-distance curves for excitation of 10-μm-diameter fibers parallel to the z axis ($\alpha = 0°$) with 100-μs current pulses in anisotropic ($\sigma_x = \sigma_y = \sigma_{xy} < \sigma_z$) and isotropic media ($\sigma_x = \sigma_y = \sigma_z$) are shown in Fig. 3(a). Both the slope and intercept of the current-distance relationship were influenced by the principal conductivities. Compared to the isotropic case, $\sigma_z/\sigma_{xy} = 1$, ratios of $\sigma_z/\sigma_{xy} < 1$ decreased the slope of the current-distance curve, whereas ratios of $\sigma_z/\sigma_{xy} > 1$ increased the slope. As in isotropic media, the larger the effective conductivity $(\sigma_z * \sigma_{xy})$ the larger the intercept. Identical trends were observed for activation of 20-μm fibers, although the absolute values were different. These data demonstrate that the threshold current to excite nerve fibers varied with the electrical conductivities along the principal axes.

To quantify the influence of anisotropy on excitation, a family of current-distance curves were generated by systematic variation of the longitudinal and transverse conductivities. The relationship between the threshold current, $I_{\text{thr-ext}}$, and the electrode to fiber distance, $(x^2+y^2+z^2)^{1/2}$, was fit

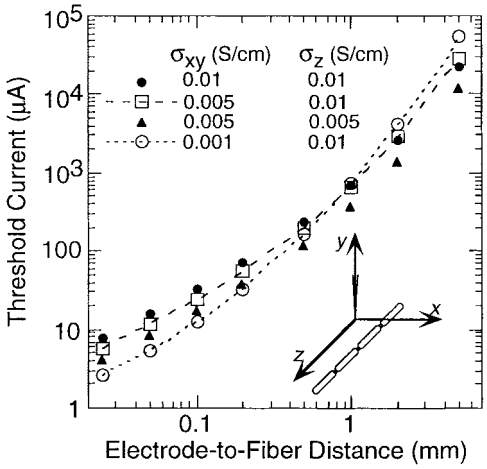

(a)

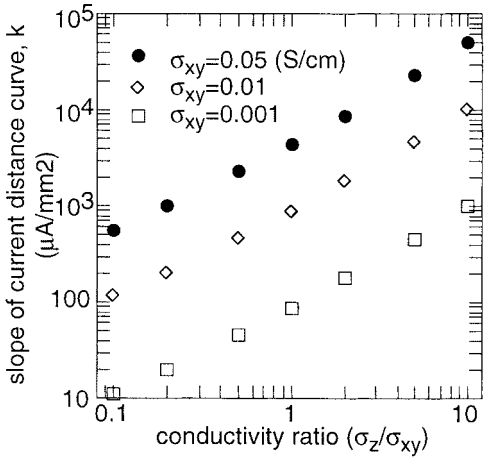

(b)

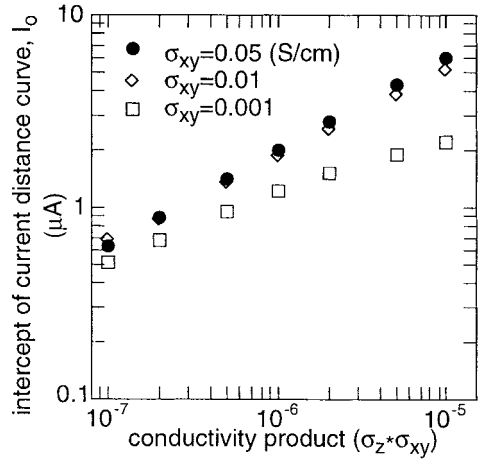

(c)

Fig. 3. Current-distance relationships in anisotropic media. (a) The relationship between the threshold current to excite a 10-μm fiber with a 100-μs current pulse and the electrode to fiber distance (current-distance curve) varied as the orthogonal conductivities were changed. The fiber lay in a plane parallel to the x-z plane, parallel to the z-axis, as shown in the inset. (b) The slope of the current-distance curve, k, was a power function of the ratio of the orthogonal conductivities (σ_{xy}/σ_z). (c) The intercept of the current-distance curve, I_o, was a power function of the product of the orthogonal conductivities $(\sigma_{xy} * \sigma_z)$.

by the equation $I_{\text{thr-ext}} = I_o + k(x^2 + y^2 + z^2)^{1/2}$ using least squares regression. The current amplitudes were logarithmically transformed before the fit to provide equal weighting of the regression error at all distances. The current-distance data were well represented by this equation, and the regression coefficient, r^2, was greater than 0.93 in all cases. The slope of the current-distance curve, k, determined the threshold difference between fibers at different distances from the electrode, and for a given longitudinal conductivity, the slope was a power function of the ratio of the orthogonal conductivities [Fig. 3(b)]. The intercept of the current-distance curve, I_o, determined the absolute threshold, and for a given longitudinal conductivity, the intercept was a power function of the product of the orthogonal conductivities [Fig. 3(c)]. Thus, the slope and intercept of the current-distance curve in anisotropic media were dependent on the ratio and product of the orthogonal conductivities, respectively.

2) Influence of Fiber Orientation on Thresholds: The threshold for excitation in anisotropic media also varied with the position of the nerve fiber relative to the principal axes. Fig. 4(a) shows the threshold for excitation of 10-μm nerve fibers lying 1 mm from the electrode as a function of the angle (α) of the fiber relative to the longitudinal (z) axis. The threshold decreased as the fiber orientation approached the less conductive (x) axis, and the decrease was larger for media with greater anisotropy. Fig. 4(b) shows the threshold difference between fibers oriented parallel $(\alpha = 0°)$ and perpendicular $(\alpha = 90°)$ to the longitudinal axis, normalized by the threshold of the parallel fibers, (i.e., $\{I_{\text{thr-ext}}[0°] - I_{\text{thr-ext}}[90°]\}/I_{\text{thr-ext}}[0°]$) as a function of the conductivity ratio. The magnitude of the threshold difference between fibers at the different orientations was dependent on the ratio of the longitudinal to transverse conductivities, such that greater anisotropy produced larger threshold differences. The threshold difference between fibers at different orientations was also dependent on the distance from the electrode. At larger electrode to fiber distances (>0.5 mm) the normalized threshold difference increased rapidly for small degrees of anisotropy, whereas anisotropy had more negligible effects at smaller electrode to fiber distances. These data demonstrate that the threshold was dependent on fiber orientation in anisotropic media.

3) Influence of Anisotropy on Recruitment Order: The dependence of threshold on fiber orientation in anisotropic media led to changes in the recruitment order of differently oriented nerve fibers with respect to both fiber diameter and electrode to fiber distance. Such differences in orientation are expected between intramuscular nerve branches and between axon collaterals throughout the central nervous system.

In anisotropic media the threshold difference between different diameter nerve fibers was dependent on the orthogonal conductivities as well as the orientation of the fibers. Fig. 5(a) shows the threshold differences between 10-μm fibers, oriented at either $\alpha = 45°$ or $\alpha = 90°$, and 20-μm fibers oriented at $\alpha = 0°$, as a function of the transverse conductivity at two different electrode to fiber distances. In strongly anisotropic media $(\sigma_z/\sigma_{xy} > 4)$ there were reversals in the recruitment order between different diameter nerve fibers oriented in

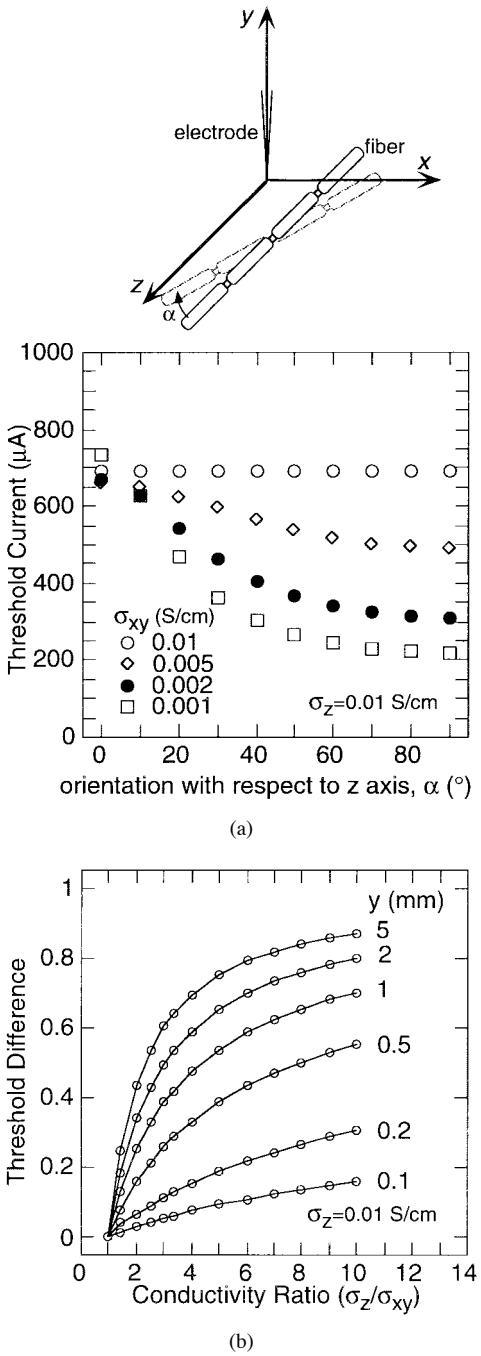

Fig. 4. The effect of fiber orientation on thresholds in anisotropic media. (a) Threshold current for excitation of a 10-μm fiber with a 100-μs current pulse in media of varying anisotropy ($\sigma_z = 0.01$ S/cm), as a function of the angle (α) of the fiber with respect to the z-axis. The electrode was positioned at the origin, the fiber lay in a plane parallel to the x-z plane at angle α to the z-axis, and the electrode to fiber distance was 1 mm. (b) Normalized threshold difference between fibers lying parallel ($\alpha = 0°$) and fibers lying perpendicular ($\alpha = 90°$) to the z-axis in media of varying anisotropy. Different curves are shown for different electrode to fiber distances, y. The electrode was positioned at the origin and both fibers lay in a plane parallel to the x-z plane.

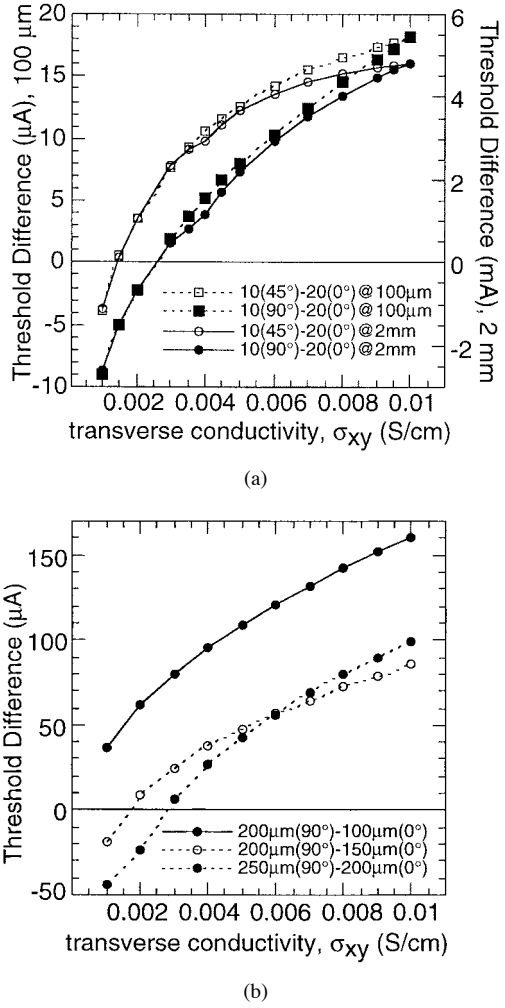

Fig. 5. Reversals of recruitment order in anisotropic media. (a) Threshold difference between 10-μm fibers, oriented at either $\alpha = 90°$ or $\alpha = 45°$, and 20-μm fibers oriented at $\alpha = 0°$, as a function of the transverse conductivity ($\sigma_{xy}, \sigma_z = 0.01$ S/cm), at two electrode to fiber distances. Electrode and fiber geometry is as in Fig. 1(a) and the stimulus was a 100-μs monophasic current pulse. (b) Threshold difference between 20-μm fibers oriented at $\alpha = 90°$ at one distance from the electrode and 20-μm fibers oriented at $\alpha = 0°$ at a closer distance from the electrode, as a function of the transverse conductivity ($\sigma_{xy}, \sigma_z = 0.01$ S/cm). Electrode and fiber geometry is as in Fig. 1(a) and the stimulus was a 100-μs monophasic current pulse.

different directions, and 10-μm fibers oriented at 45° or 90° had lower thresholds than 20-μm fibers oriented at 0°. The relative changes in the threshold difference as a function of the transverse conductivity were very similar at the two distances. Thus, anisotropy led to reversals in the recruitment order between fibers of different diameters.

Similarly, the threshold difference between nerve fibers at different distances from the electrode was dependent on the orthogonal conductivities as well as the orientation of the fibers. Fig. 5(b) shows the threshold differences between 20-μm fibers oriented at $\alpha = 90°$, at positions further from the electrode, and 20-μm fibers oriented at $\alpha = 0°$, at positions closer to the electrode, as a function of the transverse conductivity. In strongly anisotropic media, fibers that were oriented at $\alpha = 90°$ further from the electrode were stimulated at lower currents than fibers oriented at $\alpha = 0°$ closer to the electrode. The reversals in recruitment order occurred for fibers separated by 50 μm but not for fibers separated by 100 μm, and reversals occurred at lower anisotropy ratios for fibers further from the electrode. Similar, but less pronounced effects were found for 10 μm fibers, and when comparing the threshold difference between fibers oriented at $\alpha = 45°$ and fibers oriented at $\alpha = 0°$. Thus, anisotropy led to reversals

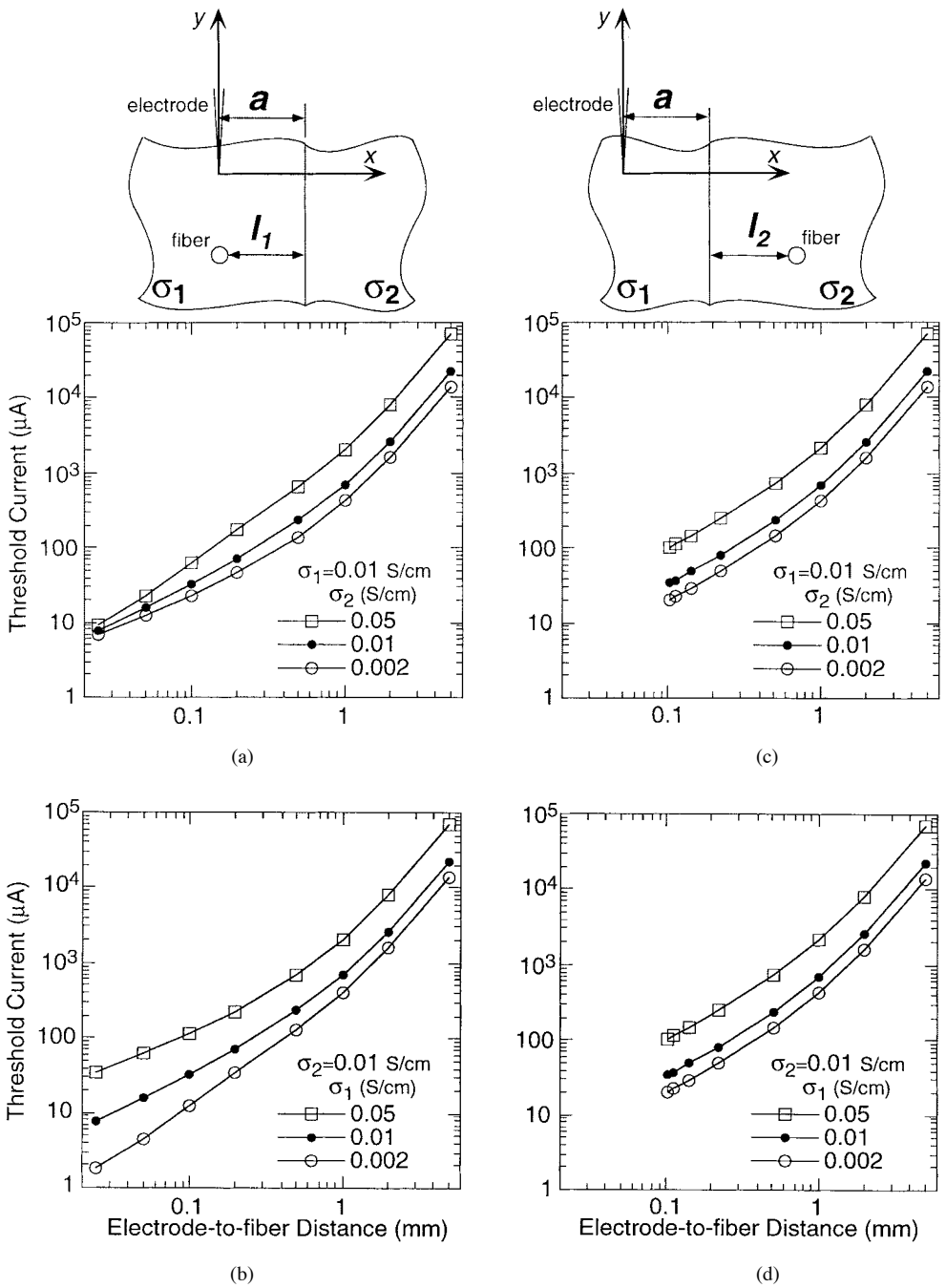

Fig. 6. Current-distance relationships in inhomogeneous media. (a), (b) Current-distance curves for excitation of 10-μm fibers in region 1 for different values of conductivity in (a) region 1 and (b) region 2. (c), (d) Current-distance curves for excitation of 10-μm fibers in region 2 for different values of conductivity in (c) region 1 and (d) region 2. In all cases the electrode was in region 1, the stimulus was a 100-μs monophasic current pulse, and the electrode, the fiber in region 1, and the fiber in region 2 were all equidistant from the interface ($a = l_1 = l_2 = 50$ μm).

in the recruitment order between fibers at different distances from the electrode.

C. Inhomogeneous Extracellular Medium

Boundaries between regions of different composition within the body create spatial inhomogeneities in the electrical conductivity of the extracellular tissue. The influence of a plane boundary between two semi-infinite isotropic media of differing conductivity [Fig. 1(b)] on patterns of nerve fiber excitation was studied for wide ranging conductivity values and electrode and nerve fiber geometries.

1) Influence of Regional Conductivity on Current-Distance Curves: Current-distance curves for excitation of fibers in regions 1 and 2 by a source in region 1 are shown in Fig. 6 for different values of the conductivity of the two regions (σ_1, σ_2). Higher values of either σ_1 or σ_2 increased the current required to excite fibers in both regions, whereas lower values of either σ_1 or σ_2 decreased the threshold current in both regions. Higher values of σ_2 increased both the intercept and slope of the current-distance curve for fibers in region 1 [Fig. 6(a)], whereas higher values of σ_1 increased the intercept but decreased the slope [Fig. 6(b)]. For fibers in region 2,

higher values of σ_2 only increased the intercept of the current-distance curve and did not affect the slope [Fig. 6(c)], whereas higher values of σ_1 increased the intercept of the current-distance curve in a manner identical to that caused by increases in σ_2 [Fig. 6(d)]. Thus, in the source free region (region 2), the current-distance curve was dependent only on the average conductivity; see (4), whereas in the region containing the source (region 1), the intercept of the current-distance curve was directly related to both σ_1 and σ_2, and the slope was directly related to σ_2 and inversely related to σ_1.

2) Influence of Electrode and Fiber Position on Current-Distance Curves: The effects of inhomogeneity on the current-distance curve were determined for different electrode and fiber positions relative to the conductivity interface. The current-distance curves for fibers in regions 1 and 2 are shown in Fig. 7 for different fiber-to-interface distances, l. In region 1, fibers closer to the interface experienced larger increases in the intercept of the current-distance curve and smaller increases in the slope of the current-distance curve as compared to fibers positioned further from the interface [Fig. 7(a)]. These effects were subtle, and were restricted to electrode positions closer to the fiber (<1 mm). Identical results were obtained by fixing the position of the fiber ($l = 50$ μm) and varying the electrode-to-interface distance, a (not shown). For fibers in region 2 the current-distance curves were independent of the position of the fiber [Fig. 7(b)] and the position of the electrode (not shown) relative to the interface, and as seen when assessing the effects of conductivity (Fig. 6), the thresholds in region 2 were only dependent on the average conductivity. These data demonstrate that the relative conductivities of the two regions had a stronger effect on excitation thresholds than did the positions of the fiber or electrode relative to the interface.

3) Influence of Inhomogeneity on Regions of Excitation: The influence of inhomogeneity on the spatial patterns of excitation is shown in Fig. 8 for three media: homogeneous, inhomogeneous with $\sigma_2 > \sigma_1$, and inhomogeneous with $\sigma_2 < \sigma_1$. The contours are lines of equal threshold, and increases in contour spacing correspond to decreases in the threshold difference between fibers at different distances from the electrode. In the homogeneous medium, the equithreshold contours were circles, were spaced uniformly, and fibers at a given distance from the electrode had equal threshold regardless of the direction [Fig. 8(a)]. In the inhomogeneous media, the threshold contours were noncircular, were nonuniformly spaced, and threshold for excitation at a given distance from the electrode was dependent on the direction from the electrode. When $\sigma_2 > \sigma_1$ the spacing between contours decreased, such that the same stimulus amplitude activated fibers over a much smaller region [Fig. 8(b)]. The greatest decrease in contour spacing (i.e., increase in threshold difference between fibers at different distances from the electrode) was observed immediately adjacent to the interface. When $\sigma_2 < \sigma_1$ the spacing between contours increased such that a larger area of tissue was activated by a given amplitude of the stimulus [Fig. 8(c)]. Although the increased area of activation spanned both regions, the decrease in threshold difference between fibers at different distances from the electrode was most pronounced immediately adjacent to the interface. The nonuniform spacing of equithreshold

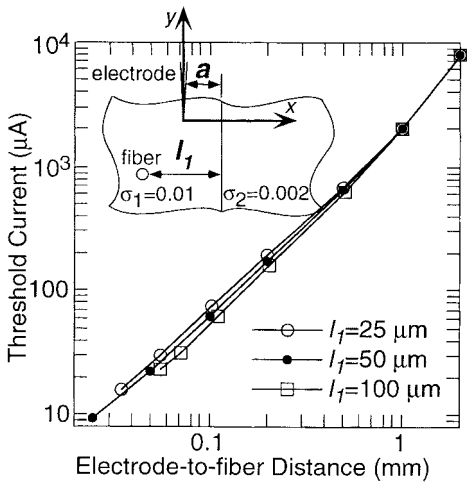

(a)

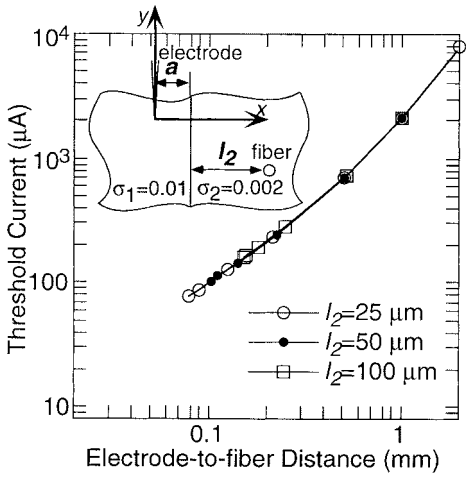

(b)

Fig. 7. Effect of the proximity of the fiber to the interface on the current-distance relationship in an inhomogeneous media ($\sigma_1 = 0.01$ S/cm, $\sigma_2 = 0.05$ S/cm). (a) Current-distance curves for excitation of 10-μm fibers in region 1 for different positions, l_1, of the fiber relative to the conductivity interface. (b) Current-distance curves for excitation of 10-μm fibers in region 2 for different positions, l_2, of the fiber relative to the conductivity interface. In all cases the electrode was in region 1, the stimulus was a 100-μs monophasic current pulse, and the electrode was 50 μm from the interface ($a = 50$ μm).

contours on either side of the conductivity interface indicated that fibers at a further distance from the electrode in one region were activated at lower current amplitudes than fibers at a closer distance to the electrode in the other region (i.e., reversals in the current-distance relationship).

4) Influence of Inhomogeneity on Recruitment Order: The changes in activation patterns in inhomogeneous media led to reversals in the recruitment order between fibers in the two regions, with respect to both fiber diameter and electrode to fiber distance. The threshold differences between 10-μm- and 20-μm-diameter fibers in the two regions, as a function of the conductivity of region 2, are shown by the open symbols in Fig. 9. In both geometries [Fig. 9(a) and (b)], the fibers in region 1 and the fibers in region 2 were equidistant from the point current source. In a homogeneous medium ($\sigma_1 = \sigma_2 = 0.01$ S/cm) the thresholds to excite fibers of the same diameter were equal, and it took more current [35

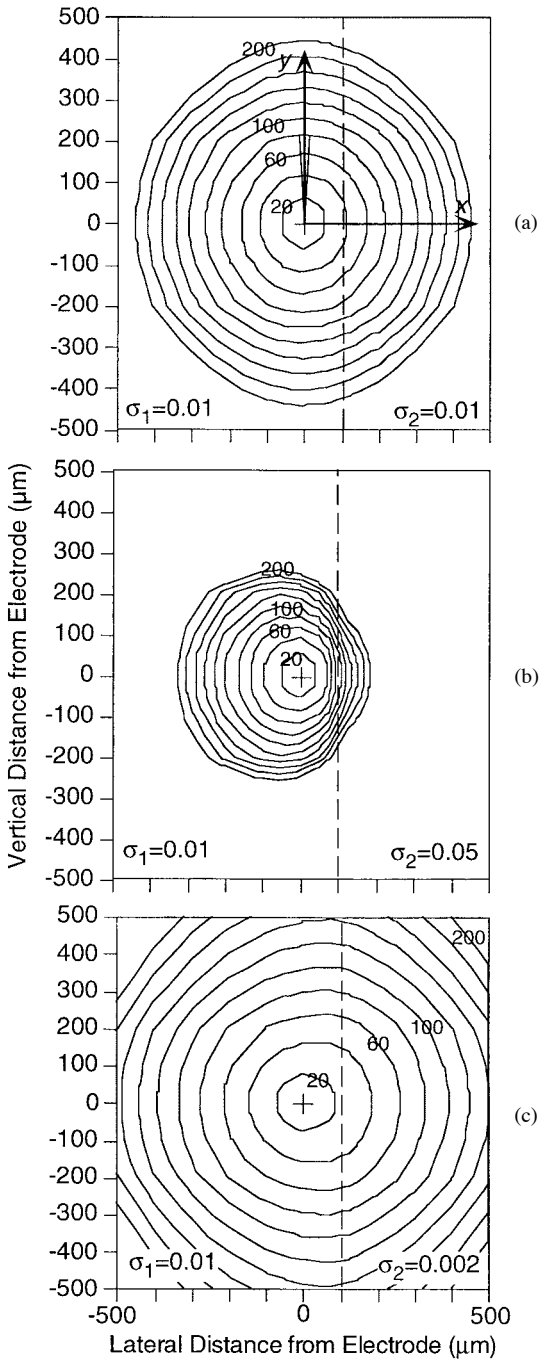

Fig. 8. Comparison of excitation regions in homogeneous and inhomogeneous media. Each plot shows contours of equal threshold for activation of 10-μm-diameter fibers with a 100-μs monophasic current pulse. The electrode and fiber geometry are as shown in Fig. 1(b) with $a = 100$-μm. (a) homogeneous medium with $\sigma_1 = \sigma_2 = 0.01$ S/cm. (b) inhomogeneous medium $\sigma_1 = 0.01$ S/cm and $\sigma_2 = 0.05$ S/cm. (c) inhomogeneous medium with $\sigma_1 = 0.01$ S/cm and $\sigma_2 = 0.002$ S/cm. In all cases, the location of the electrode is indicated by the +, the location of the interface is indicated by the vertical dashed line, and the contours are spaced at 20-μA increments.

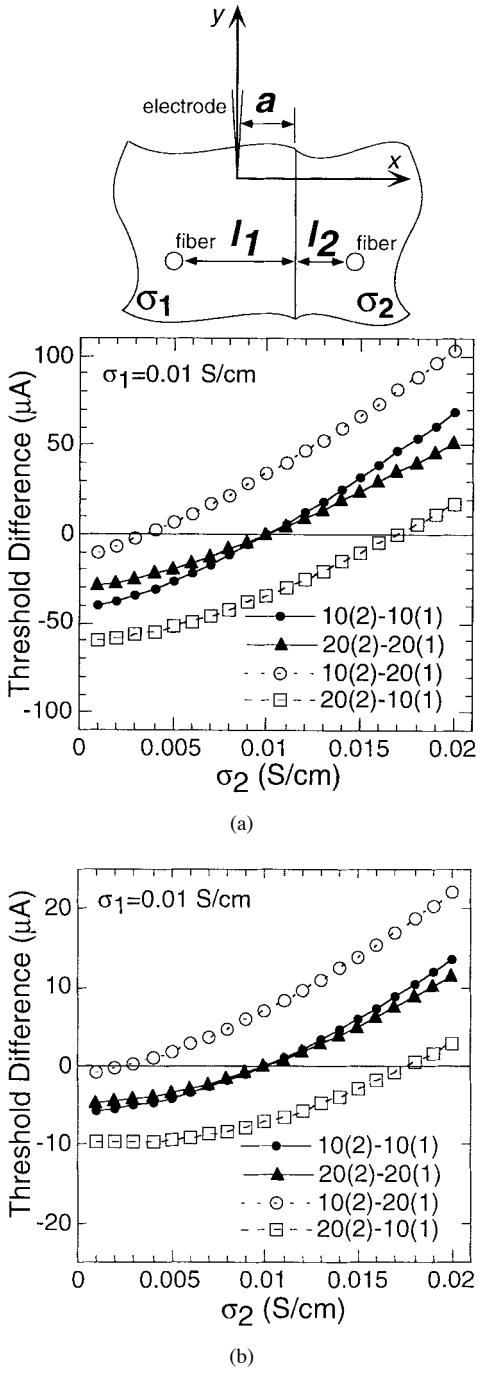

Fig. 9. Reversals of recruitment order in inhomogeneous media. (a), (b) Threshold differences between fibers in region 2 and fibers in region 1 as a function of the conductivity in region 2. The fibers in region 1 and region 2 were equidistant from the electrode in both geometries: (a) $l_1 = 600$ μm, $l_2 = a = 200$ μm, $y = -200$ μm, (b) $l_1 = 150$ μm, $l_2 = a = 50$ μm, $y = -50$ μm. The stimulus was a 100 μs monophasic current pulse and $\sigma_1 = 0.01$ S/cm.

μA in (a), 8 μA in (b)] to excite the 10-μm fibers than the 20 μm fibers. In an inhomogeneous medium with $\sigma_2 \sim 0.1 * \sigma_1$, the 10-$\mu$m fibers in region 2 had lower thresholds than the 20 μm fibers in region 1. Similarly, with $\sigma_2 \sim 2 * \sigma_1$, the 10-$\mu$m fibers in region 1 had lower thresholds than the 20-μm fibers in region 2. Thus, when comparing recruitment in regions of different conductivity, there were reversals in the recruitment order such that smaller diameter fibers were activated with less current than required to activate larger diameter fibers.

Similarly, there were reversals in the recruitment order between fibers at different distances from the electrode. The threshold differences between fibers of the same diameter at the same distance from the electrode but in different regions are shown by the filled symbols in Fig. 9. In a homogeneous

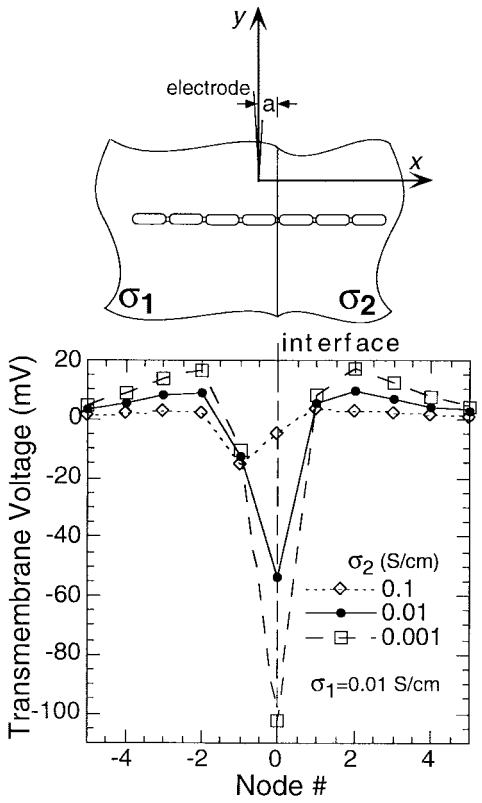

Fig. 10. Profiles of transmembrane potential in inhomogeneous media. The transmembrane potential at the 11 central nodes of a 10-μm-diameter nerve fiber crossing the plane interface between media of differing conductivity for different values of the conductivity in region 2 (σ_2). In all cases $\sigma_1 = 0.01$ S/cm, the stimulus was a 100-μs monophasic current pulse, and the geometry is shown at the top with $a = 250$ μm, $y = -500$ μm, and the interface (indicated by the dashed line) coincident with node 0.

medium ($\sigma_1 = \sigma_2 = 0.01$ S/cm) the thresholds to excite fibers of the same diameter at the same distance from the electrode were equal. However, in inhomogeneous media, the threshold to excite a given fiber was strongly dependent on the regional conductivity. When region 2 was less conductive than region 1 ($\sigma_2 < \sigma_1$), the fibers in region 2 had lower thresholds than the fibers in region 1, whereas when region 2 was more conductive than region 1 ($\sigma_2 > \sigma_1$), the fibers in region 2 had higher thresholds than the fibers in region 1. These data demonstrate that when comparing excitation of fibers in regions of differing conductivity, reversals in recruitment order with respect to the electrode to fiber distance occurred, and thus the distance from the electrode over which fibers are activated by a given current will vary between regions of different conductivity.

5) Fibers Crossing the Conductivity Interface: Inhomogeneity in the extracellular medium also influenced the excitation patterns of fibers crossing between media. Changes in the profile of the transmembrane potential along the fibers and reversals in the recruitment order between 10-μm and 20-μm fibers resulted from differences in the conductivity of the two regions. An example of the effect of the conductivity interface on transmembrane potential is shown in Fig. 10. When σ_2 was increased from 0.01 S/cm to 0.1 S/cm the location of the most depolarized node (i.e., the site of action potential initiation) shifted from node 0 to node -1, and the location of the most hyperpolarized node shifted from node 2 to node 1. Decreases in σ_2 to 0.001 S/cm did not result in a shift of either the most depolarized node or the most hyperpolarized node for the geometries that were studied. The effects of the inhomogeneity on fibers crossing the conductivity interface were smaller for closer electrode to fiber distances. With the electrode 100 μm from the fiber, the spatial profile of polarization along the fibers was altered, but no shifts in excitation site were found when σ_2 was increased from 0.01 S/cm to 0.1 S/cm. With the electrode 200 μm from the fiber, increasing σ_2 from 0.01 S/cm to 0.1 S/cm resulted in a shift by 1 node in the location of the most depolarized node in the 10-μm fiber.

The recruitment order between different diameter nerve fibers crossing the conductivity interface was dependent on the conductivities of the two regions. When σ_2 was increased from 0.01 S/cm to 0.1 S/cm, less current was required to excite 10-μm fibers than 20-μm fibers for electrode to fiber distances of 500 μm. Decreases in σ_2 to 0.001 S/cm did not alter the recruitment order between large and small fibers for the geometries that were studied. These results demonstrate that spatial inhomogeneity in the extracellular conductivity can influence the site of excitation and the relative thresholds for fibers crossing the conductivity interface.

IV. Discussion

The electrical conductivity of biological tissues is, in general, inhomogeneous and often anisotropic [12], [14]. The results of this simulation study demonstrate that the electrical properties of the extracellular medium can have a strong influence on the pattern of neuronal excitation generated by extracellular electric fields.

A. Methodological Considerations

Analytical solutions to Poisson's equation were used to calculate the extracellular potentials generated by a point current source in various media, which spanned the range of conductivities encountered in biological tissues [12], [14]. It was assumed that the anisotropic media behaved as a monodomain (i.e., that no current crossed the membranes of the elements that created the anisotropy). The advantage of this assumption was that it allowed analytical calculation of extracellular potentials using a coordinate transformation [29], [52]. The monodomain assumption is valid for bundles of myelinated nerve fibers (e.g., peripheral nerve, central tracts) where the high impedance of the myelin restricts the amount of current that can cross the membrane [1], [3]. However, the monodomain assumption is probably less accurate for tissues such as skeletal muscle where the membrane allows appreciable current flow throughout its length [33], [42], [44]. The redistribution of current from the extracellular space to the intracellular space will alter the magnitude and distribution of transmembrane potentials, and thus affect the patterns of excitation generated in these tissues.

A model of two semi-infinite homogenous isotropic media joined at a plane boundary was used to calculate the potentials in an inhomogeneous medium. The two region model enabled a closed-form solution for the potential with a single image

source. More complex models with multiple layers may be more appropriate for certain tissues, and lead to solutions with infinite numbers of image sources [30]. For this study, however, such a model would have made difficult the systematic variation of conductivity and geometric parameters to examine their influence on excitation. Many biological tissues are probably both inhomogeneous and anisotropic. However, analytical solutions for such geometries place restrictions on the directions of the anisotropy [26], and a numerical solution for such a geometry was beyond the scope of this investigation.

The net driving function, which provides a closed form solution for the transmembrane potential in a passive nerve fiber, was used to predict excitation thresholds [53]. Although the model was passive, the nonlinear conductance properties of neural membrane [6], [48] were incorporated in the strength-duration curve used to predict threshold [53]. The high impedance myelin sheath was assumed to be a perfect insulator [27], [43]. This assumption will have the effect of decreasing the chronaxie time as compared to the case of finite impedance myelin [43]. The presence of the fiber was also assumed not to affect the potentials generated by the extracellular electrode, an assumption that has been previously verified [27], [35].

The relationship between the threshold current, $I_{\text{thr-ext}}$, and the electrode to fiber distance, $(x^2 + y^2 + z^2)^{1/2}$, was modeled as $I_{\text{thr-ext}} = I_o + k(x^2 + y^2 + z^2)^{1/2}$. Previous experimental results have demonstrated that this provides a good description of the current-distance relationship [4], [5], [40], [46], [21], [54], and this equation fit the data well. The intercept, I_o, determined the absolute threshold, and the slope, k, determined the threshold difference between fibers at different distances from the electrode.

B. Implications

In anisotropic media, representative of bundles of nerve fibers or skeletal muscle (σ_z/σ_{xy} as high as 10), the slope of the current-distance curve increased as compared to a homogeneous medium. The same intensity stimulus would therefore activate a smaller region of tissue than predicted by an isotropic model (i.e., smaller number of fibers), and larger increases in current would be required to activate additional fibers. In anisotropic media, thresholds were strongly dependent on the orientation of the fibers relative to the principal axes. The dependence of threshold on orientation is important when considering activation of different motor nerve branches within a skeletal muscle [10], [17]. For example, discontinuities in input-output properties were previously attributed to recruitment of motor nerve branches lying at different distances from the electrode, but the present results demonstrate that an equally plausible explanation is that the branches had different orientations within the muscle. Differences in orientation are also important when considering activation of axon collaterals within the central nervous system [24], [25]. Importantly, the effect of orientation on threshold in anisotropic media could be minimized by decreasing the electrode to fiber distance [Fig. 4(b)].

In source-free regions of semi-infinite, inhomogeneous media (two regions separated by a plane boundary), the intercept of the current-distance relationship was dependent only on the average conductivity, and the slope was independent of the conductivities. Thus, recruitment in this region was predicted accurately by a homogeneous model with conductivity equal to the average conductivity of the two media. In regions containing the source, the pattern of excitation was strongly dependent on the electrical conductivities of both regions, and recruitment could not be predicted with the homogeneous model. Inhomogeneous media resulted in reversals in the recruitment order between fibers of differing diameter and at different distances from the electrode. These results have implications for studies employing extracellular stimulation of cells in inhomogeneous media, and particularly those that have used threshold measurements to determine neural structure [25].

V. Conclusion

The results of this simulation study demonstrate that the electrical properties of the extracellular medium can have a strong influence on the pattern of neuronal excitation generated by extracellular electric fields. Spatial variations in electrical properties, as present in biological tissues, generated nonintuitive shifts in the pattern of excitation. Inhomogeneity in the electrical conductivity of the extracellular tissue caused reversals in the recruitment order between different diameter fibers and between fibers at different distances from the electrode. Similarly, in strongly anisotropic media there were reversals in the recruitment order between different diameter fibers and between fibers at different distances from the electrode. Such reversals may lead to erroneous interpretations of activation patterns if it is assumed that recruitment order is the same as that predicted in an isotropic homogeneous medium. Thus, interpretation of studies using electrical stimulation to activate a groups of neurons requires consideration of the local tissue electrical properties. The results also point to the importance of using anatomically and electrically accurate models to predict patterns of excitation in complex volume conductors.

Acknowledgment

The author would like to thank Dr. C. L. Van Doren for reviewing an earlier version of the manuscript.

References

[1] K. W. Altman and R. Plonsey, "Analysis of the longitudinal and radial resistivity measurements of the nerve trunk," *Ann. Biomed. Eng.*, vol. 17, pp. 313–324, 1989.
[2] K. W. Altman and R. Plonsey, "Analysis of excitable cell activation: Relative effects of external electrical stimuli," *Med. Biol. Eng. Comput.*, vol. 28, pp. 574–580, 1990a.
[3] K. W. Altman and R. Plonsey, "Point source nerve bundle stimulation: Effects of fiber diameter and depth on simulated excitation," *IEEE Trans. Biomed. Eng.*, vol. 37, pp. 688–698, 1990b.
[4] E. V. Bagshaw and M. H. Evans, "Measurement of current spread from microelectrodes when stimulating within the nervous system," *Exp. Brain Res.*, vol. 25, pp. 391–400, 1976.
[5] S. L. BeMent and J.B. Ranck, A quantitative study of electrical stimulation of central myelinated fibers," *Exp. Neurol.*, vol. 24, pp. 147–170, 1969.
[6] S. Y. Chiu, J. M. Ritchie, R. B. Rogart, and D. Stagg, "A quantitative description of membrane currents in rabbit myelinated nerve," *J. Physiol.*, vol. 292, pp. 149–166, 1979.
[7] B. Coburn, "A theoretical study of epidural electrical stimulation of the spinal cord-Part II: Effects on long myelinated fibers," *IEEE Trans. Biomed. Eng.*, vol. BME-32, pp. 978–986, 1985.

[8] B. Coburn, "Neural modeling in electrical stimulation," *CRC Crit. Rev. Biomed. Eng.*, vol. 17, pp. 133–178, 1989.
[9] B. Coburn and W. K. Sin, "A theoretical study of epidural electrical stimulation of the spinal cord-Part I: Finite element analysis of stimulus fields," *IEEE Trans. Biomed. Eng.*, vol. BME-32, pp. 971–977, 1985.
[10] P. E. Crago, P. H. Peckham, and G. B. Thrope, Modulation of muscle force by recruitment during intramuscular stimulation," *IEEE Trans. Biomed. Eng.*, vol. BME-27, pp. 679–684, 1980.
[11] C. C. Finley, B. S. Wilson, and M. W. White, "Models of neural responsiveness to electrical stimulation," in *Cochlear Implants: Models of the Electrically Stimulated Ear.*, J. M. Miller and F. A Spelman, Eds. New York: Springer-Verlag, 1990, pp. 55–96.
[12] K. R. Foster and H. P. Schwan, "Dielectric properties of tissues and biological materials: A critical review," *CRC Crit. Rev. Biomed. Eng.*, vol. 17, pp. 25–104, 1989.
[13] J. H. M. Frijns, S. L. de Snoo, and R. Schoonhoven, "Potential distributions and neural excitation patterns in a rotationally symmetric model of the electrically stimulated cochlea," *Hearing Res.*, vol. 87, pp. 170–186, 1995.
[14] L. A. Geddes and L. E. Baker, "The specific resistance of biological material—A compendium of data for the biomedical engineer and physiologist," *Med. Biol. Eng.*, vol. 5, pp. 271–293, 1967.
[15] F. L. H. Gielen, W. Wallinga-de Jonge, and K. L. Boon, Electrical conductivity of skeletal muscle tissue: experimental results from different muscles in vivo," *Med. Biol. Eng. Comput.*, vol. 22, pp. 569–577, 1984.
[16] P. H. Gorman and J. T. Mortimer, "The effect of stimulus parameters on the recruitment characteristics of direct nerve stimulation," *IEEE Trans. Biomed. Eng.*, vol. BME-30, pp. 407–414, 1983.
[17] P. A. Grandjean and J. T. Mortimer, "Recruitment properties of monopolar and bipolar epimysial electrodes," *Ann. Biomed. Eng.*, vol. 14, pp. 53–66, 1986.
[18] W. M. Grill, "Effects of tissue electrical properties on neural excitation," in *Proc. 18th Annu. Int. Conf. IEEE Engineering in Medicine and Biology Society*, Amsterdam, the Netherlands, 1996.
[19] W. M. Grill and J. T. Mortimer, "The effect of stimulus pulse duration on selectivity of neural stimulation," *IEEE Trans. Biomed. Eng.*, vol. 43, pp. 161–166, Feb. 1996.
[20] W. M. Grill and J. T. Mortimer, "Inversion of the current-distance relationship by transient depolarization," *IEEE Trans. Biomed. Eng.*, vol. 44, pp. 1–9, Jan. 1997.
[21] B. Gustafsson and E. Jankowska, "Direct and indirect activation of nerve cells by electrical pulses applied extracellularly," *J. Physiol.*, vol. 258, pp. 33–61, 1976.
[22] P. B. Hoeltzell and R. W. Dykes, "Conductivity in the somatosensory cortex of the cat-evidence for cortical anisotropy," *Brain Res.*, vol. 177, pp. 61–82, 1979.
[23] J. Holsheimer, "Electrical conductivity of the hippocampal CA1 layers and application to current source density analysis," *Exp. Brain Res.*, vol. 67, pp. 402–410, 1987.
[24] J. Holsheimer, J. J. Struijk, and N. R. Tas, "Effects of electrode geometry and combination on nerve fiber selectivity in spinal cord stimulation," *Med. Biol. Eng. Comput.*, vol. 33, pp. 676–682, 1995.
[25] E. Jankowska and W. J. Roberts, "An electrophysiological demonstration of the axonal projections of single spinal interneurons in the cat," *J. Physiol.*, vol. 222, pp. 597–622, 1972.
[26] I. V. Lindell, K. I. Nikoskinen, and M. J. Flykt, "Electrostatic image theory for an anisotropic half-space slightly deviating from transverse anisotropy," *Radio Sci.*, vol. 31, pp. 1361–1368, 1996.
[27] D. R. McNeal, "Analysis of a model for excitation of myelinated nerve," *IEEE Trans. Biomed. Eng.*, vol. BME-23, pp. 329–337, 1976.
[28] P. W. Nicholson, "Specific impedance of cerebral white matter," *Exp. Neurol.*, vol. 13, pp. 386–401, 1965.
[29] P. W. Nicholson, "Experimental models for current conduction in an anisotropic medium," *IEEE Trans. Biomed. Eng.*, vol. BME-14, pp. 55–56, 1967.
[30] P. L. Nunez, "Electric fields of the brain The neurophysics of EEG." New York: Oxford Uni. Press, New York, pp. 454–457, 1981.
[31] Y. C. Okada, J.-C. Huang, M. E. Rice, D. Tranchina, and C. Nicholson, "Origin of the apparent tissue conductivity in the molecular and granular layers of the in vivo turtle cerebellum and the interpretation of current source-density analysis," *J. Neurophysiol.*, vol. 72, pp. 742–753, 1994.
[32] L. W. Organ and H. C. Kwan, "Electrical impedance variation along a tract of brain tissue," *Ann. N.Y. Acad. Sci.*, vol. 170, pp. 491–508, 1970.
[33] A. Peskoff, "Electric potential in three-dimensional electrically syncytial tissues," *Bull. Math. Biol.*, vol. 41, pp. 163–181, 1979.
[34] R. Plonsey, *Bioelectric Phenomena*. New York: McGraw Hill, 1969.
[35] R. Plonsey and R. C. Barr, "Electric field stimulation of excitable tissue," *IEEE Trans. Biomed. Eng.*, vol. 42, pp. 329–336, 1995.
[36] R. Plonsey and D. Heppner, "Considerations of quasi-stationarity in electrophysiological systems," *Bull. Math. Biophys.*, vol. 29, pp. 657–664, 1967.
[37] J. B. Ranck Jr. and S. L. BeMent, "The specific impedance of the dorsal columns of the cat: an anisotropic medium," *Exp. Neurol.*, vol. 11, pp. 451–463, 1965.
[38] F. Rattay, "Analysis of models for extracellular fiber stimulation," *IEEE Trans. Biomed. Eng.*, vol. 36, pp. 676–681, 1989.
[39] J. P. Reilly, V. T. Freeman, and W. D. Larkin, "Sensory effects of transient electrical stimulation-evaluation with a neuroelectric model," *IEEE Trans. Biomed. Eng.*, vol. BME-34, pp. 752–754, 1985.
[40] W. J. Roberts and D. O. Smith, "Analysis of threshold currents during microstimulation of fibers in the spinal cord," *Acta Physiol. Scand.*, vol. 89, pp. 384–394, 1973.
[41] P. N. Robillard and Y. Poussart, "Specific-impedance measurements of brain tissues," *Med. Biol. Eng. Comput.*, vol. 15, pp. 438–445, 1977.
[42] B. J. Roth, F. L. H. Gielen, and J. P Wikswo Jr., "Spatial and temporal frequency-dependent conductivities in volume-conduction calculations for skeletal muscle," *Math. Biosci.*, vol. 88, pp. 159–189, 1988.
[43] J. T. Rubinstein, "Analytical theory for extracellular electrical stimulation of nerve with focal electrodes II: Passive myelinated axon," *Biophys. J.*, vol. 60, pp. 538–555, 1991.
[44] N. G. Sepulveda, B. J. Roth, and J. P. Wikswo Jr., "Current injection into a two-dimensional anisotropic bidomain," *Biophys. J.*, vol. 55, pp. 987–999, 1989.
[45] W. K. Sin and B. Coburn, "Electrical stimulation of the spinal cord: A further analysis relating to anatomical factors and tissue properties," *Med. Biol. Eng. Comput.*, vol. 21, pp. 264–269, 1983.
[46] S. D. Stoney Jr., W. D. Thompson, and H. Asanuma, "Excitation of pyramidal tract cells by intracortical microstimulation: Effective extent of stimulating current," *J. Neurophysiol.*, vol. 31, pp. 659–669, 1968.
[47] J. J. Struijk, J. Holsheimer, B. K. van Veen, and H. B. K. Boom, "Epidural spinal cord stimulation: Calculation of field potentials with special reference to dorsal column nerve fibers," *IEEE Trans. Biomed. Eng.*, vol. 38, pp. 104–110, 1991.
[48] J. D. Sweeney, D. Durand, and J. T. Mortimer, "Modeling of mammalian myelinated nerve for functional neuromuscular stimulation," in *Proc. 9th Annu. Int. Conf. IEEE Engineering in Medicine and Biology Society*, 1987, pp. 1577–1578.
[49] I. Tasaki, "A new measurement of action currents developed by single nodes of Ranvier," *J. Neurophysiol.*, vol. 27, pp. 1199–1206.
[50] P. H. Veltink, J. A. van Alste, and H. B. K. Boom, "Influences of stimulation conditions on recruitment of myelinated nerve fibers: A model study," *IEEE Trans. Biomed. Eng.*, vol. 35, pp. 917–924, 1988.
[51] P. H. Veltink, J. A. van Alste, and H. B. K. Boom, "A modeling study of nerve fascicle stimulation," *IEEE Trans. Biomed. Eng.*, vol. 36, pp. 683–691, 1989.
[52] J. R. Wait, "Current flow into a three-dimensionally anisotropic conductor," *Radio Sci.*, vol. 25, pp. 689–694, 1990.
[53] E. N. Warman, W. M. Grill, and D. Durand, "Modeling the effects of electric fields on nerve fibers: Determination of excitation thresholds," *IEEE Trans. Biomed. Eng.*, vol. 39, pp. 1244–1254, 1992.
[54] J. Yeomans, P. Prior, and F. Bateman, "Current-distance relations of axons mediating circling elicited by midbrain stimulation," *Brain Res.*, vol. 372, pp. 95–106, 1986.

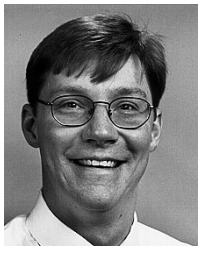

Warren M. Grill, Jr. (S'88–M'95) was born in Plainfield, NJ, in 1967. He received the B.S. degree in biomedical engineering, with honors, in 1989 from Boston University, Boston, MA. He received the M.S. degree in 1992 and the Ph.D. degree in 1995, both in biomedical engineering, from Case Western Reserve University, Cleveland, OH. During the summer of 1995 he attended the Neural Systems and Behavior course at the Marine Biological Laboratory, Woods Hole, MA, with an NIH-NRSA fellowship.

Dr. Grill is presently Elmer L. Lindseth Assistant Professor of Biomedical Engineering at Case Western Reserve University and a Principal Investigator of the Cleveland FES Center. His research interests include neural prostheses, the electrical properties of tissues and cells, computational neuroscience, and neural control.

Dr. Grill is a member of the Biomedical Engineering Society, the IEEE Engineering in Medicine and Biology Society, and the Society for Neuroscience. He is a Founding Member of the International Functional Electrical Stimulation Society and currently sits on its Board of Directors. While a graduate student, he received awards for conference papers from the IEEE-EMBS and RESNA.